JOURNAL OF APPLIED ELECTROCHEMISTRY 23 (1993) 1223–1231

Analysis of spontaneous electrochemical noise for corrosion studies

P. R. ROBERGE

Department of Chemistry & Chemical Engineering, Royal Military College of Canada, Kingston, Ontario, K7K 5LO, Canada

Received 20 October 1992; revised 20 January 1993

Spontaneous electrochemical noise can be a rich source of information concerning the processes simultaneously occurring at a corroding interface. But the combination of deterministic and stochastic events which make up noise signatures is often complicated by the specific nature of the systems being investigated. This paper describes a study of voltage noise fluctuations recorded during the free corrosion of commercial aluminium sheet material and compares typical results obtained with different noise analysis techniques.

1. Introduction

The study of spontaneous current or potential fluctuations for the characterization of corrosion processes has received considerable attention in recent years. But the study of chemical oscillations in general and electrochemical fluctuations in particular has always fascinated scientists. The early work published in the field of fluctuating electrochemical systems was reviewed in 1972 by Tyagai [1], in 1987 by Bezegh and Janata [2] and in 1988 by Searson and Dawson [3].

The expression 'electrochemical noise' (EN), in a corrosion context, has been applied to both current fluctuations between two similar metallic specimens and to the corrosion potential fluctuations that can be recorded between such corroding specimens and a reference electrode [4–7]. While the measurement of current noise has recently gained some popularity because it apparently follows in intensity the actual corrosion rates [6, 7], the fluctuations of the corrosion potential in free corroding situations will always remain a phenomenon rich in information about the heterogeneous corrosion processes themselves. The study of such fluctuations for the characterization of a corroding interface has an important advantage over all other electrochemical techniques since it is completely non perturbative.

The study of corrosion potential fluctuations was applied, for example, to monitor the onset of events characterizing pitting [8–11] or stress corrosion cracking corrosion [12–15]. Understanding the chronology of the initial events related to these forms of corrosion is a fundamental component of the science interested in studying localized corrosion. During localized corrosion electrochemical noise seems to be generated by both stochastic processes typically present during passivation breakdown and repassivation events, and deterministic processes such as film formation or pit propagation.

Stochastic models of processes occurring at an electrochemical interface have been developed to describe various components of these processes. The derivation of a model to describe the stochastic nature of the charge transfer between a metallic surface and an electrolyte can be made on the general theory of fluctuations in non-equilibrium physicochemical systems [11]. Blanc *et al.* [16] proposed in 1977 a model of electrochemical reaction fluctuations based on a Langevin description where the elementary noise sources consists of a white noise influx acting directly on fluxes of particles. More recently a study [4] made with iron specimens exposed to an inhibited (200 p.p.m. $NaNO_2$) saline solution concluded that the potential fluctuations observed during the first few hours of pitting corrosion could be simulated with an electrochemical model consisting of four fundamental steps, (i) pit nucleation, (ii) pit growth, (iii) growth termination and (iv) repassivation. The stochastic nature of steps (i) and (iii) was an essential component of the model proposed in this study.

In the present paper fluctuations of the corrosion potential observed on freely corroding sheet aluminium material exposed to aerated saline solutions will be analysed with new noise analysis techniques based on the stochastic nature of the directional changes of the recorded voltage corresponding to voltage peaks observed throughout the exposure periods. The study of corroding aluminium specimens is particularly suited for the development and testing of new noise analysis techniques since such corrosion, which is often very localized, has already been the subject of extensive studies by many other researchers [8, 17–23].

2. Noise analysis

The most common way to analyse noise data has been to transform time records in the frequency domain in

0021-891X

order to obtain power spectral density (PSD) plots. Since noise signals can be produced by either deterministic or stochastic processes and often consist of a complex combination of these processes, the most universal analytical approach has been to correlate predominant frequencies and deconvolute unwanted signals in an iterative manner using well established mathematical functions [24, 25]. Spectral density plots would thus be computed utilizing fast Fourier transforms (FFT) or other algorithms such as the maximum entropy method (MEM) [26, 27].

Although some investigators argue that features of the PSD curves [28, 29], such as the slope of the decaying power with frequency at some characteristic frequencies, can be related to corrosion rates, it remains that much useful information is lost when real time data is converted into the frequency domain. While these techniques find a very appropriate use for the deconvolution of spectroscopic data sets which often contain millions of data points, they can yield disappointing results when these averaging procedures are applied to smaller sets of data points. The utilization of approximations as in the MEM technique to circumvent this limitation will itself be affected by the presence of non-stationary phenomena which can greatly complicate the final analysis.

Two relatively new approaches for the characterization of random or partially random noise signatures were compared in the present study. The first technique consisted in transforming voltage or signal fluctuations into individual peaks as basic events [9]. Each directional change of the slope of the recorded voltage was used as a trigger and the resulting inter-event times (peak duration) compiled in a histogram type distribution. The rise time (dV/dt) of the voltage peaks was also evaluated since such a parameter could be an important characteristic of electrochemical systems. The subsequent analysis of the peak population was itself imported from the field of statistics of event series such as practiced in reliability engineering [30]. Situations in which discrete events occur randomly in a continuum (e.g. time) and which are called stochastic point processes can normally be described by a Poisson probability distribution $p(x; \lambda t)$, as in Equation 1, where x represents a random variable, t the specific time involved and $1/\lambda$ the mean number of events per unit time.

$$p(x;\lambda t) = \frac{(\lambda t)^x}{x!}\, e^{(-\lambda t)} \qquad x = 0, 1, 2, \ldots \quad (1)$$

For situations where the hazard rate is constant ($x = 0$), the Poisson probability distribution can be reduced [31] to an exponential distribution (Equation 2) where the mean number of occurence ($1/\lambda$) can be obtained by integrating the occurrence distribution of the phenomena present in a given sample.

$$f(t) = \lambda e^{(-\lambda t)} \quad (2)$$

After the voltage fluctuations have been sorted into peak population distributions and then plotted as cumulative distributions (Equation 3) from which the characteristic parameter λ can be evaluated at a point of the cumulative distribution given by Equation 4 which corresponds to a computerized version of the classical method of finding λ by plotting data on exponential distribution probability papers.

$$F(t) = \sum \frac{\text{Histogram}(t)}{\sum \text{Histogram}(t)} \quad (3)$$

$$\sum_{t=1}^{1/\lambda} \frac{\text{Histogram}(t)}{\sum \text{Histogram}(t)} = 0.6321 \quad (4)$$

The second approach to analyze the voltage fluctuations was derived from one of the most useful mathematical models for analyzing time-series data which was proposed a few years ago by Mandelbrot and van Ness [32]. Although the fractional Brownian motion (fBm) model can help to describe very complex geometries or time series, its analysis can be made relatively simply by using the rescaled range analysis technique which was originally proposed by Hurst [33] and applied by Mandelbrot and Wallis to the determination of the fractal characteristics of a time series [34]. A detailed description of the rescaled range analysis or R/S technique (where R or $R(t, s)$ stands for the sequential range of the data points increments for a given lag s and time t, and S or $S(t, s)$ for the square root of the sample sequential variance) can be found in Fan *et al.* [35]. Hurst [33] and later Mandelbrot and Wallis [34] have proposed that the ratio $R(t, s)/S(t, s)$, also called the rescaled range, is itself a random function with a scaling property described by Relation 5 where the scaling behaviour of a signal is characterized by the Hurst exponent (H) which can vary between $0 < H < 1$,

$$\frac{R_{(t,s)}}{S_{(t,s)}} \propto S^H \quad (5)$$

It has additionally been shown [36] that the local fractal dimension $d_{F\ell}$ of a fBm noise trace is related to H through Equation 6 which makes it possible to characterize the fractal dimension of given time series by simply calculating the slope of a R/S plot.

$$d_{F\ell} = 2 - H, \qquad 0 < H < 1 \quad (6)$$

3. Experimental details

The specimens were cut from commercial 2024-T3 sheet material (thickness 1.0 mm; nominal composition Si: 0.5, Fe: 0.5, Cu: 4.3, Mn: 0.6, Mg: 1.5, Zn: 0.25) to appropriate sizes for mounting in epoxy according to metallographic techniques. The samples were mounted in a manner that would expose only one face of each of three orthogonal planes that were related to the rolling direction of the sheet. Henceforth, these faces will be called the rolled surface, the long transverse edge (with its long axis parallel and its short axis perpendicular to the rolling direction) and the short transverse edge (with both long and short axes perpendicular to the rolling

direction), respectively. Prior to mounting, provisions were made for electrical connection to the unexposed back of the samples and the unexposed edges were coated with an aluminium–vinyl anti-corrosive paint to prevent crevice corrosion between the epoxy mount and the aluminium electrodes. After mounting, the specimens were polished (using 240, 400 and finally 600 grit papers) and cleaned with dichloromethane.

For each experiment, a pair of identical aluminium specimens (same exposed face) were immersed in a $2\,dm^3$ beaker containing a solution of 3% sodium chloride. Each cell was equipped with an air purge and a saturated calomel electrode (SCE) brought into close proximity with one electrode by a Luggin probe. The mounted specimens were separated by 2.5 mm and kept in a stable parallel position with plastic holders.

The electrochemical impedance spectroscopy (EIS) measurements were performed with a commercial generator/analyser (Solartron model 1255) at the corrosion potential and always taken in the direction of decreasing frequency. Each measurement was repeated five times in order to ascertain the stability of the system being evaluated. A frequency range of 100 to 0.1 Hz was selected for its sensitivity to corrosion resistance. A potentiostat was not used in these measurements. The alternating current was applied directly between the two aluminium electrodes and kept at a value which would not cause more than 10 mV difference (peak to peak) across the cell. The polarization resistance values (R_p) were determined automatically, during these experiments, with the projection of centres analysis technique described elsewhere [37–39].

The reference electrode (SCE) served to measure the corrosion potential and its fluctuations. The fluctuations themselves were monitored through a high pass filter (1 mΩ resistor in parallel to a 1 μF capacitor with a lower frequency cut-off (f_c) at 0.16 Hz) in order to increase the sensitivity of the measurement technique. The high sensitivity multimeter used in these studies (Hewlett Packard model 3457A) had a resolution of 10 nV on its most sensitive scale (30 mV). A sampling interval (Δt) of 0.5 s and a number of consecutive data points (N) of 1800 were chosen since this would give a factual measuring frequency window where corrosion processes are dominant [3, 18]. The frequency domain corresponding to these sampling conditions can be evaluated to be between 1 Hz (f_{max}) and 1 mHz (f_{min}) with the help of Equations 7 and 8 [29]. But since the use of a high-pass filter in these studies will have affected the shapes and amplitudes of the voltage fluctuations differently depending on their relation with the cut-off frequency f_c (unaffected above f_c and as dV/dt under f_c) the information extracted from the lower frequency domain can only be used comparatively.

$$f_{max} = \frac{1}{2\Delta t} \tag{7}$$

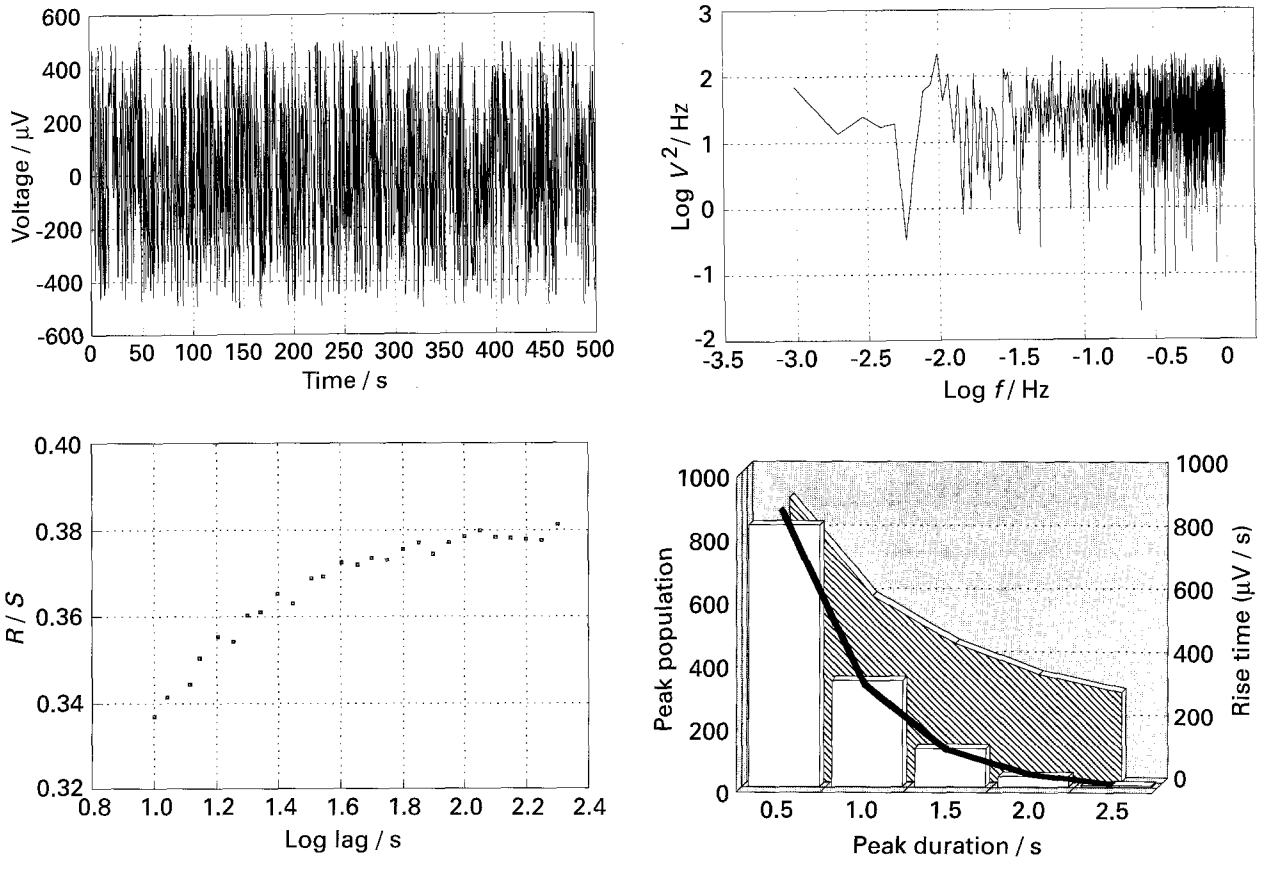

Fig. 1. Typical white noise file (a) and its results of analysis by FFT (b), with the R/S technique (c) and the SPD technique (d).

$$f_{\min} = \frac{1}{N\Delta t} \tag{8}$$

A custom-made multiplexer controlled by a laboratory computer (Hewlett Packard model 86A) directed the inputs from each technique to a storage device. At the completion of these experiments, the specimens were removed and examined with optical microscopy to observe differences in corrosion morphologies.

4. Results and discussion

The noise analysis techniques considered in the present study were tested with synthetic noise files generated with simple algorithms based on random generator functions [40]. Figure 1 illustrates the results obtained when a typical white noise file (Fig. 1(a)) was analysed by FFT (Fig. 1(b)), with the R/S technique (Fig. 1(c)) and with the stochastic pattern detector (SPD) technique (Fig. 1(d)). The absence of slope observed on the PSD representation of FFT analysis of this white noise file is matched by a small curvature present in the high frequency (short lags) end of the equivalent R/S plot. Such a distortion is common when the lag values approach the sampling frequency itself. It should be noted that the values on the R/S scale of the R/S plot (Fig. 1(c)) are greatly magnified and that the total curvature only corresponds to approximately 20% of the levelling values observed at higher lag values (lower frequencies). The corresponding analysis of the white noise file by SPD (Fig. 1(d)) is characterized by an almost perfect exponential decay of the peak population/peak duration histogram which is translated in this specific case by a correlation coefficient of 99.1% between synthesized data and the exponential decay calculated with the global $1/\lambda$ value (1.0) calculated for this file.

Another characteristic worth noting in Fig. 1(d) is the decaying values of rise time as a function of the peak population calculated for this white noise file. This phenomenon would reflect both the decreasing probability of finding subsequent peaks with increasing amplitude and the normalization of the rise time parameter by the peak duration itself. When a Brownian motion noise file (Fig. 2(a)) was analysed by FFT, its PSD plot (Fig. 2(b)) was characterized by a slope of 2 typical of $1/f^2$ noise. The $1/f^2$ behaviour was also revealed on the R/S plot (Fig. 2(c)) where a slope of 0.5 is related to the exponent (β) of the $1/f^{\beta}$ expression by Equation 9 [40].

$$\beta = 2H + 1 \tag{9}$$

The analysis of the same Brownian motion noise file by SPD (Fig. 2(d)) produced an almost perfect fit (correlation coefficient 99.2%) between the noise data and the expected decay of purely random processes but the global $1/\lambda$ value (1.5) calculated for this file was larger than for a white noise file. By experimenting with real files with R/S slopes H of various intermediate values (between 0 and 0.5) a simple relation was found between the average decay

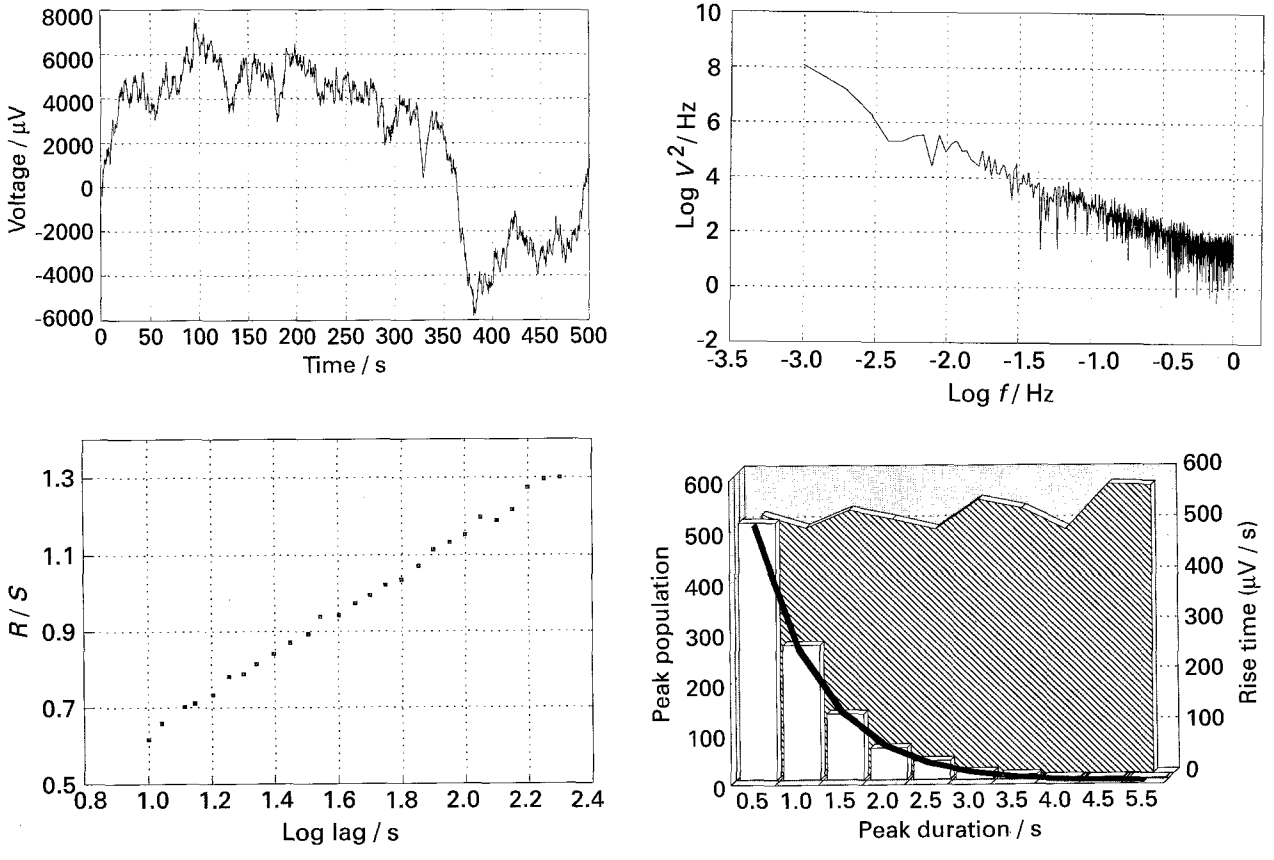

Fig. 2. Typical Brownian motion noise file (a) and its results of analysis by FFT (b), with the R/S technique (c) and the SPD technique (d).

coefficient λ and the Hurst exponent (Equation 10).

$$H = 1/\lambda - 1 \qquad \text{for } 0 < H < 0.5 \qquad (10)$$

It could also be demonstrated, in this effort to correlate the results obtained with the different noise analysis techniques, that the presence of persistence [35] in noise files, which is translated by higher values of H and λ, affects each technique quite differently, the SPD technique being very sensitive to the presence of deterministic features in a noise signal. It should also be noted that the rise time curve (Fig. 2(d)) obtained with Brownian motion noise is independent of peak duration values. While this characteristic has not been exploited any further during the present study, it is felt that it could eventually be used to separate different corrosion modes that may be simultaneously present in noise signatures.

The voltage fluctuations observed during the corrosion of aluminium specimens exposed to aerated saline solutions was also used to illustrate the differences and similarities between the results obtained with different noise analysis techniques. Twenty-two noise files recorded at regular intervals during the two week exposure period of rolled 2024-T3 surfaces were analysed by the R/S technique and a map of the relative results of analysis is presented in Fig. 3 where three regions can be readily identified. In the first region (file 1 to 6), the R/S slope values for the short lags are very close to 0.5, which is typical of Brownian motion noise, and diminish for higher lag values. The few very dark spots in this first region could indicate the presence of persistence at the frequencies corresponding to the lag values on the abscissa of Fig. 3.

The second region of this plot (file 7 to file 14) seems to be almost totally characterized by the presence of anti-persistence [35] (R/S slope < 0.5) which would correspond to fBm noise signatures with an exponent β between 2 and 1 i.e. between Brownian motion and the very common $1/f$ behaviour. The third region in Fig. 3 is itself characterized by very variable R/S slope values that vary between subsequent files in repetitive patterns. This would indicate the presence of persistence at specific frequencies for the rest of this experiment.

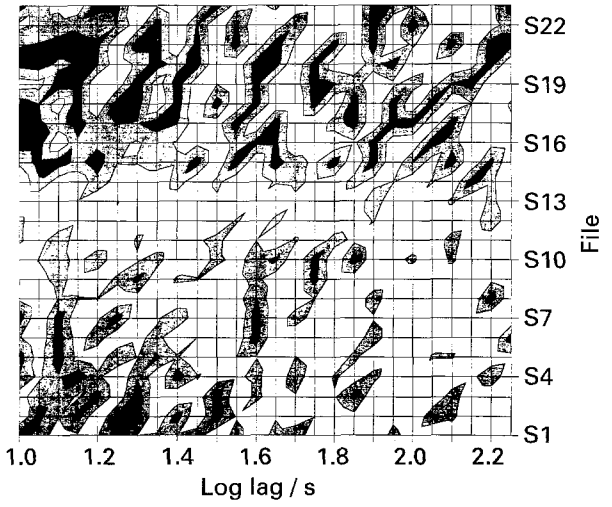

Fig. 3. Results of analysis by the R/S technique of twenty-two noise files obtained at regular intervals during the two week exposure of 2024-T3 sheet material in an aerated saline solution (white, $R/S < 0.48$; grey, $0.48 < R/S < 0.68$; black, $R/S > 0.68$).

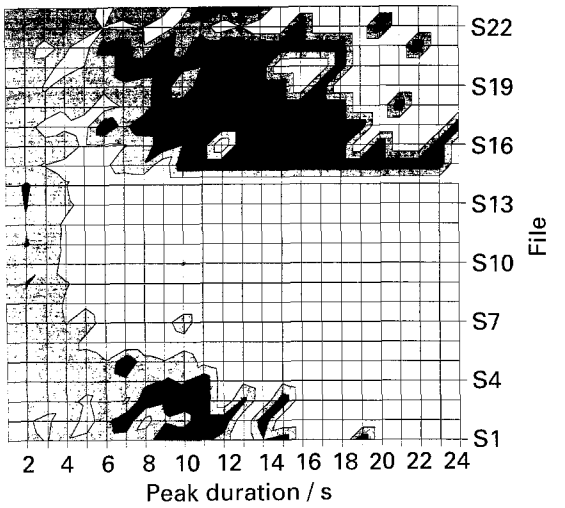

Fig. 4. Results of analysis by the SPD technique of twenty-two noise files obtained at regular intervals during the two week exposure of 2024-T3 sheet material in an aerated saline solution (white, real < 0.8 model; grey, 0.8 model < real < 1.2 model; black, real > 1.2 model).

A similar treatment of the results obtained by analysing the same noise files with SPD is presented in Fig. 4. The threshold values which served to rank the results in this case were based on the adherence to the exponential decay model by the real data once transformed into peak duration vs peak population histograms. Experimental values agreeing with the exponential decay model within 20% of the predicted values have a grey shade in this plot (Fig. 4) while they are either white when smaller or black when larger. Such a procedure can efficiently highlight the presence of longer peaks which would be more predominant when deterministic processes are controlling the corrosion reactions. The three regions visible in Fig. 3 were repeated in Fig. 4 where the presence of a dark area around the 10 s peak duration is quite visible for the first 4 measurements. The extensive presence of persistence also became very visible at noise file 15 and lasted until the end of this experiment. These three regions characterized by both P/S and SPD analysis could be thought to correspond to three distinct modes controlling the corrosion of the rolled 2024 aluminium surfaces. Three original noise data files were selected to illustrate how these files would appear either in real time or after their transformation by the more classical FFT analysis.

An example typical of the first region identified in Figs 3 and 4 and presented in Fig. 5(a) (file 2, sampled at the end of first day of exposure) clearly possesses the long peaks apparent in the SPD analysis and which caused the persistence highlighted by the R/S analysis. The frequency domain where these peaks are dominant seems to be around or even below the

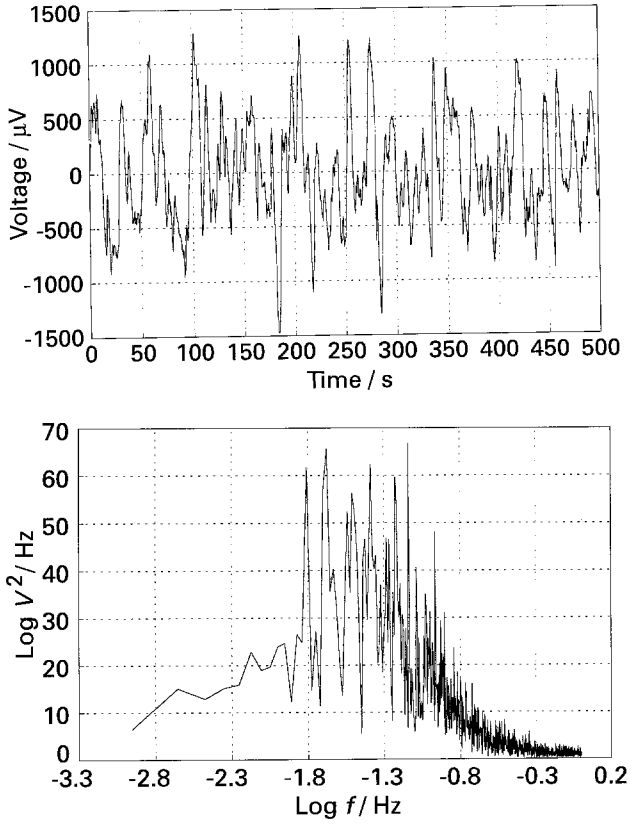

Fig. 5. A 500 s sample (a) of a noise file (file 2) acquired at the end of the first day of exposure of 2024 aluminium sheet material in an aerated saline solution and its FFT PSD plot (b).

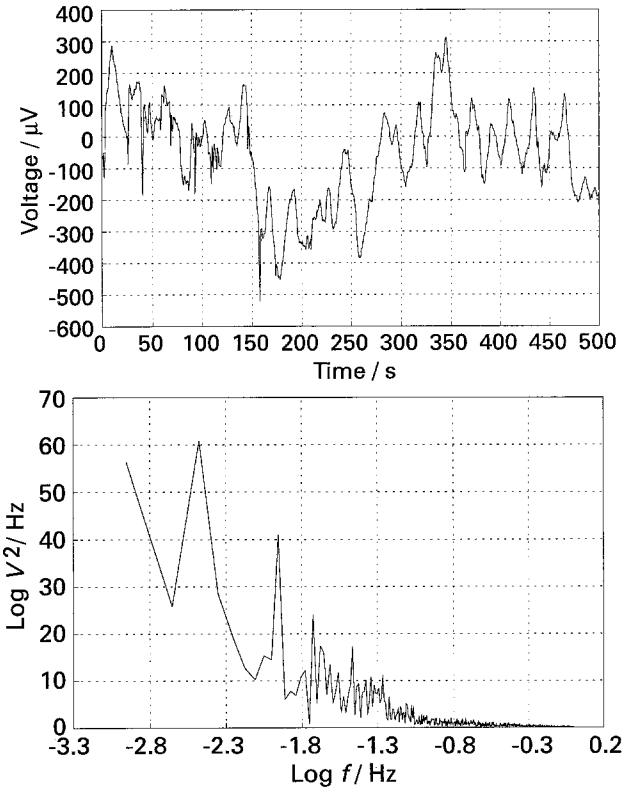

Fig. 7. A 500 s sample (a) of noise file (file 15) acquired at day 8 of exposure of 2024 aluminium sheet material in an aerated saline solution and its FFT PSD plot (b).

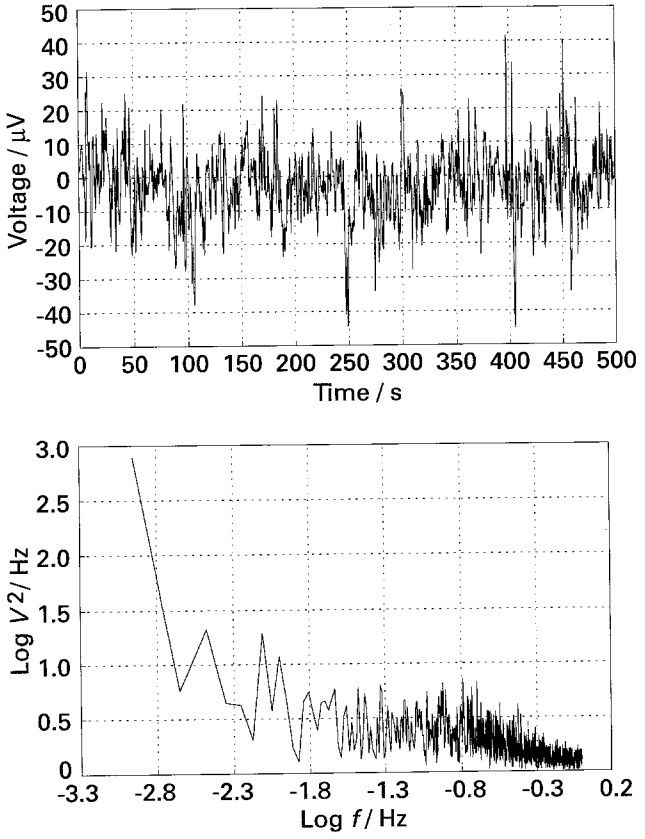

Fig. 6. A 500 s sample (a) of a noise file (file 8) acquired at the end of the third day of exposure of 2024 aluminium sheet material in an aerated saline solution and its FFT PSD plot (b).

cut-off frequency of the high-pass filter used in this study i.e. between 16 and 160 mHz on the PSD plot (Fig. 5(b)) of the FFT results obtained with this file. A typical file of the second region identified previously (file 8, end of third day of exposure) is presented in Fig. 6(a). It apparently possesses some of the features found in white noise files with a cumulating element that is characteristic of Brownian motion noise. But the results obtained by analysing this file by FFT (Fig. 6(b)) do not match either the features present in PSD plots of white noise (Fig. 1(b)) or Brownian motion noise (Fig. 2(b)). It is possible to distinguish on the PSD plot of Fig. 6(b) a stronger frequency component at approximately the cut-off frequency (160 mHz). This dominance seemed to be displaced toward lower frequencies as can be seen in the results of analysing a file of the third region (Fig. 7(a), file 15 taken at day eight) by FFT (Fig. 7(b)). In fact the presence of the high-pass filter is hardly visible on this last PSD plot, indicating that the voltage fluctuations during this period belong entirely to the low frequency domain.

While the significance of all the information that can be extricated from the extensive analysis of corrosion noise records is difficult to appreciate without more advanced modelling of the simultaneous processes occurring at these highly complex alloy-interface systems, it is possible to seek some practical and useful relations of a simpler nature. Figure 8 illustrates how the corrosion rate values, obtained by analysing the EIS results obtained during this

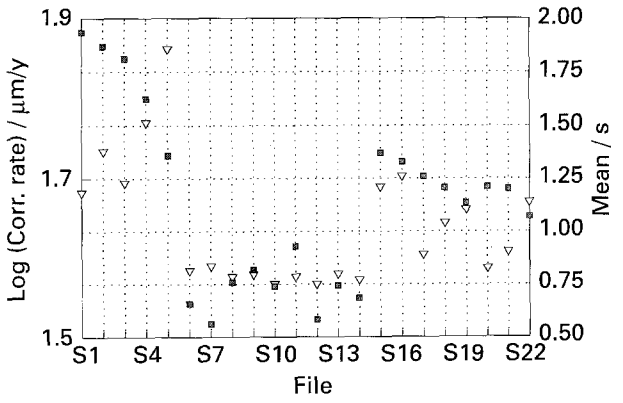

Fig. 8. Corrosion rates (■) calculated from EIS results during 10 day exposure to an aerated saline solution of rolled 2024 sheet material and mean number of events (▼) obtained by analysing the corresponding noise files with the SPD technique.

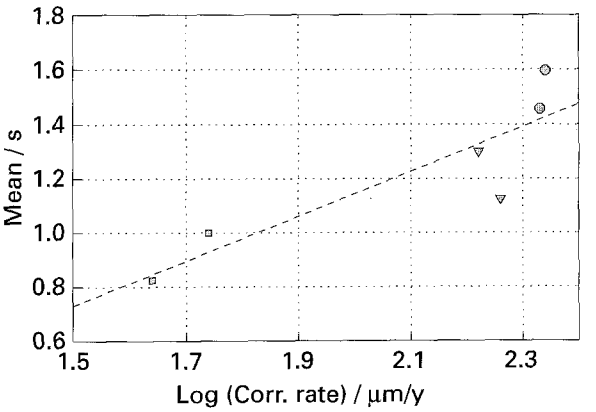

Fig. 10. Average corrosion rates and mean number of events for rolled (■), long (▼) and short (●) faces of commercial 2024 sheet material exposed during a 10 day period to aerated saline solutions.

experiment with a 2024 rolled surface, compared with the mean number of events ($1/\lambda$) calculated from the corresponding noise files. Some typical EIS results are presented in their Bode plot format (Fig. 9) to illustrate the pertinence of analysing these results with the projection of centres technique since a unique and depressed ($\log(Z)/\log(f) < 1.0$) *RC* behaviour is clearly visible in the frequency range used in this study. The three regions which were identified during the analysis of twenty-two noise files and which are still apparent in the mean number of events, were also clearly present when the corrosion rate behaviour was plotted. The initial high corrosion rates ($> 60\,\mu$m/y) calculated during the period corresponding to noise files 1 to 5 dropped considerably during the following days belonging to the second region (files 6 to 14, $\approx 35\,\mu$m/y) and finally climbed to reach intermediate values in a third and last region (files 15 and beyond, $\approx 45\,\mu$m/y).

This relation between the mean number of events obtained from noise files and the corrosion rates measured independently by EIS also held for the other experiments carried out during this study of the 2024 sheet material resistance to aerated saline solutions. The average values obtained for these two parameters during six 10 day exposure experiments involving the three faces of this commercial material is presented in Fig. 10 where the correlation coefficient between the two parameters was calculated to be 0.88. Incidentally, the average corrosion rate which was estimated from these six experiments ($117\,\mu$m/y) agrees relatively well with what was reported in the literature [41] ($139\,\mu$m/y) for similar experiments involving weight loss measurements by a 2024-T4 alloy exposed for the same period to slightly more concentrated (3.5% NaCl) saline solutions. The micrographs presented in Fig. 11 illustrate the extent of corrosion damage felt by each face of the aluminium sheet material. In this figure it can be seen that the average size of the pits formed on the three faces of the 2024-T3 sheet material increased from the rolled (16μm, Fig. 11(a)) to the long (22μm, Fig. 11(b)) and short transverse faces (28μm, Fig. 11(c)) thus confirming the corrosion ranking observed by both EIS measurements and EN monitoring.

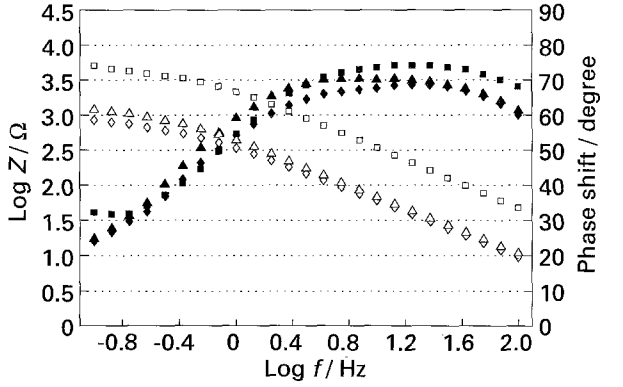

Fig. 9. EIS bode plots of impedance (white) and phase shift (black) of 2024-T3 sheet material from EIS results obtained after 6 days exposure to an aerated 3% NaCl solution: (□) rolled, (△) long, (◇) short.

5. Conclusions

The analysis of spontaneous electrochemical noise generated during the corrosion of metallic specimens can be made by various analysis techniques to reveal the stochastic and fractal nature of the simultaneous phenomena which occur at a corroding interface. The results obtained with two relatively new approaches which can be used for the characterization of random or partially random noise signatures have been compared with the results of their transformation by FFT. It has been demonstrated that both the R/S and SPD techniques can serve to highlight features present in the frequency domain of transformed data records. The usefulness of using the SPD technique for the analysis of corrosion noise became quite apparent when the mean number of events calculated with this technique was compared with corrosion rates monitored in parallel with EIS. Those encouraging results will serve as a sound basis to pursue the study of the more deterministic or chaotic features which construct electrochemical noise signatures.

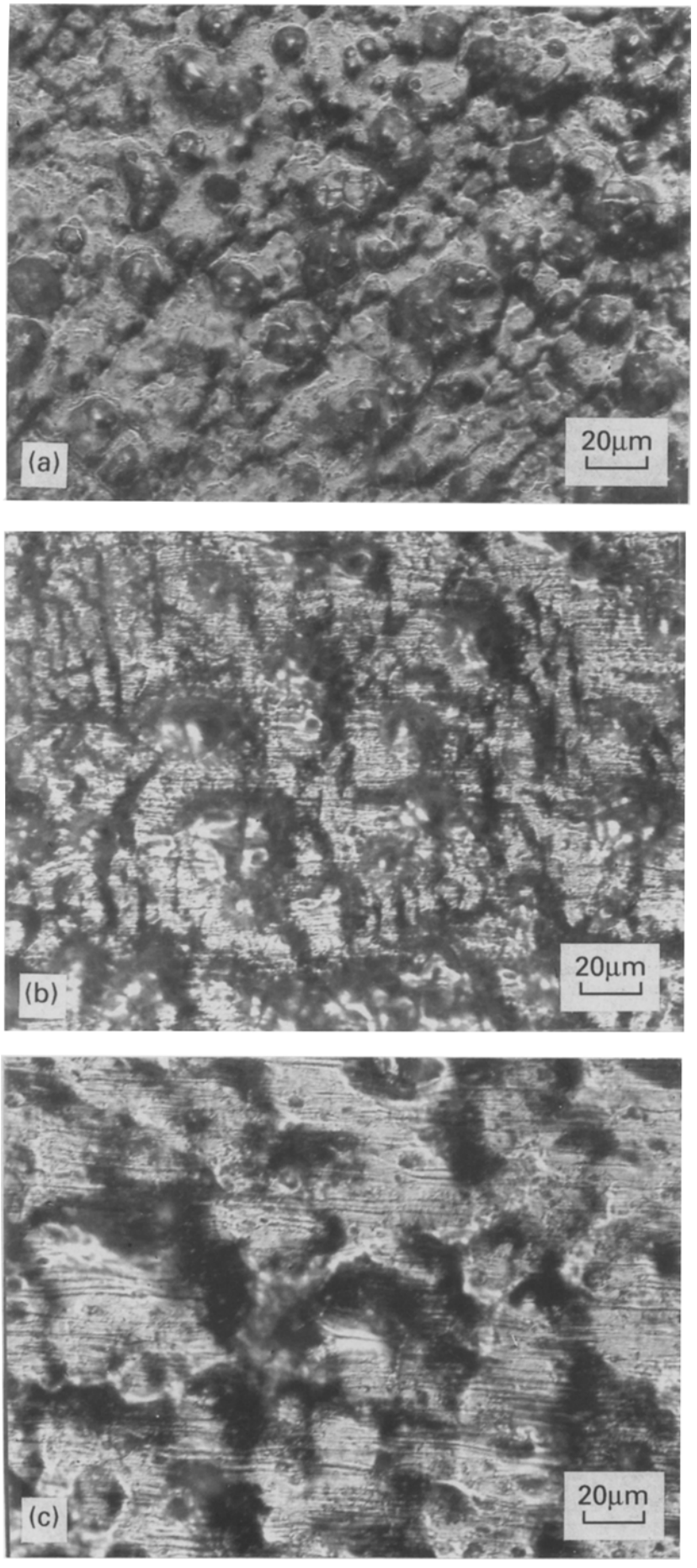

Fig. 11. Micrographs of 2024-T3 sheet material after two weeks in 3% NaCl aerated solutions: (a) rolled, (b) long and (c) short transverse faces.

Acknowledgement

The author is grateful to the Defence Research Establishment Pacific and particularly to Dr Derek Lenard without whose support this work would not have been done.

References

[1] V. A. Tyagai, *Elektrokhimiya* **10** (1974) 3.
[2] A. Bezegh and J. Janata, *Anal. Cehm.* **59** (1987) 494A.
[3] P. C. Searson and J. L. Dawson, *J. Electrochem. Soc.* **135** (1988) 1908.
[4] M. Hashimoto, S. Miyajima and T. Murata, *Corros. Sci.* **33** (1992) 885.
[5] K. Hladky, J. L. Dawson, *ibid.* **21** (1981) 317.
[6] A. N. Rothwell and D. A. Eden, 'Electrochemical Noise Techniques for Determining Corrosion Rates and Mechanisms,' CORROSION 92, Paper 223, National Association of Corrosion Engineers, Houston, TX (1992).
[7] J. B. Lumsden, M. W. Kendig and S. Jeanjaquet, 'Electrochemical Noise for Carbon Steel in Sodium Chloride Solutions-Effects of Chloride and Oxygen Activity,' CORROSION 92, Paper 224, National Association of Corrosion Engineers, Houston, TX (1992).
[8] C. Monticelli, G. Brunoro, A. Frignani and G. Trabanelli, *J. Electrochem. Soc.* **139** (1992) 706.
[9] P. R. Roberge, E. Halliop and V. S. Sastri, *Mat. Sci. Forum* **111/112** (1992) 167.
[10] C. Gabrielli, F. Huet, M. Keddam and R. Oltra, *Corrosion* **46** (1990) 266.
[11] C. Gabrieele, F. Huet and M. Keddam, *Electrochim. Acta* **31** (1986) 1025.
[12] R. A. Cottis and C. A. Loto, *Corrosion* **46** (1990) 12.
[13] C. A. Loto and R. A. Cottis, *B. Electrochem.* **4** (1988) 1001.
[14] R. C. Newman and K. Sieradzki, *Scripta Metall.* **17** (1983) 621.
[15] A. Benzaid, C. Gabrielli, F. Huet, M. Jerome and F. Wenger, *Mat. Sci. Forum* **111/112** (1992) 167.
[16] G. Blanc, J. Epelboin, C. Gabrielli and M. Keddam, *J.* Electrochem. Soc. **75** (1977) 97.
[17] W. P. Iverson, *ibid.* **115** (1968) 617.
[18] K. Hladky and J. L. Dawson, *Corros. Sci.* **22** (1982) 231.
[19] S. Magaino, M. Yasuda and H. Yamada, *Boshoku Gijutsu* **34** (1985) 157.
[20] S. Magaino, *ibid.* **34** (1985) 657.
[21] U. Bertocci, *J. Electrochem. Soc.* **127** (1980) 1931.
[22] U. Bertocci and J. Kruger, *Surface Sci.* **101** (1980) 608.
[23] U. Bertocci, *J. Electrochem. Soc.* **128** (1981) 520.
[24] E. O. Brigham, 'The Fast Fourier Transform', Prentice-Hall, Englewoods Cliffs, NJ (1974).
[25] J. S. Bendat and A. G. Piersol, 'Random Data: Analysis and Measurement Procedures', 2nd edn., John Wiley & Sons, New York (1986).
[26] N. Andersen, 'Modern Spectrum Analysis', IEEE, New York (1978).
[27] N. Andersen, *Geophysics* **39** (1974) 69.
[28] Nachstedi and K. E. Heusler, *Electrochim. Acta* **33** (1988) 311.
[29] J. C. Uruchurtu and J. L. Dawson, *Corrosion* **4** (1987) 19.
[30] P. D. T. O'Connor, 'Practical Reliability Engineering', 2nd edn., John Wiley & Sons, New York (1989).
[31] R. E. Walpole and R. H. Myers, 'Probability and Statistics for Engineers and Scientists', 4th edn., MacMillan, New York (1989).
[32] B. B. Mandelbrot and J. W. van Ness, *SIAM Review* **10** (1968) 422.
[33] E. H. Hurst, Methods of Using Long-term Storage in Reservoirs, *Proc. Inst. Civ. Eng.* **5** Part I (1956) 519.
[34] B. B. Mandelbrot and J. R. Wallis, *Water Resources Res.* **5** (1969) 321.
[35] L. T. Fan, D. Neogi and M. Yashima, 'Elementary Introduction to Spatial and Temporal Fractals', Springer-Verlag, Berlin (1991).
[36] J. Feder, 'Fractals', Plenum, New York (1988).
[37] P. R. Roberge and R. Beaudoin, *J. Appl. Electrochem.* **18** (1988) 101.
[38] P. R. Roberge, E. Halliop, M. Asplund and V. S. Sastri, *J. Appl. Electrochem.* **20** (1990) 1004.
[39] P. R. Roberge, E. Halliop and V. S. Sastri, *Corrosion* **48** (1992) 447.
[40] H. -O. Peitzen and D. Saupe, 'The Science of Fractal Images', Springer-Verlag, New York (1988).
[41] W. J. D. Shaw, *Proc. 16th Annual Tech. Intl. Metall. Soc. IMS*, AMS Metals Park, OH (1985).